C. R. Mecanique 342 (2014) 79–84

Contents lists available at ScienceDirect

Comptes Rendus Mecanique

www.sciencedirect.com

Exact geometric theory for flexible, fluid-conducting tubes

Théorie géométriquement exacte des tuyaux souples avec écoulement interne

François Gay-Balmaz [a,*], Vakhtang Putkaradze [b]

[a] *LMD – École normale supérieure de Paris – CNRS, 75005 Paris, France*
[b] *Department of Mathematical and Statistical Sciences, University of Alberta, Edmonton, AB T6G 2G1, Canada*

ARTICLE INFO

Article history:
Received 13 November 2013
Accepted 6 January 2014
Available online 28 January 2014

Keywords:
Fluid–structure interactions
Flexible tubes
Garden hose instability
Geometrically exact models
Variational principles

Mots-clés :
Interaction fluide–structure
Tuyaux souples
Instabilité du tuyau d'arrosage
Modèles géométriquement exacts
Principes variationels

ABSTRACT

Instability of flexible tubes conducting fluid, or "garden hose instability", is a phenomenon both familiar from everyday life and important for applications, which has been actively studied. However, previous works did not consider one of the most crucial physical effects — the dynamical change of the cross-section. We show how to consistently address this issue by coupling the geometrically exact rod dynamics with the fluid motion via the use of a constrained Hamilton's variational principle. We find strong effect of this dynamics on stability, and derive a variety of exact nonlinear solutions of traveling-wave type.

RÉSUMÉ

L'instabilité des tuyaux souples avec écoulement interne, ou « instabilité du tuyau d'arrosage », est un phénomène commun, étudié de longue date, et qui a d'importantes applications. Cependant, les travaux antérieurs ne tiennent pas compte d'un effet crucial : la dynamique de la section transversale du tube. Nous montrons comment l'inclure dans la dynamique en utilisant un principe de Hamilton avec contrainte, couplant la dynamique d'une tige géométriquement exacte et celle de l'écoulement interne. Nous prouvons que cela affecte l'instabilité et calculons une classe de solutions exactes de type ondes progressives.

1. Introduction

The phenomenon of instability of a tube carrying a fluid, also known as "garden hose instability", has been an object of active research because of its familiarity from everyday life, the fundamental questions it poses, and its practical importance. A theory of this phenomenon incorporating the dynamics of the combined motion of the tube and the fluid was developed starting from the 1950s [1,3]. The continuous theory consequently derived in [14] started a steady and active stream of studies in the area, with large portion of the contributions coming from Païdoussis and collaborators. We refer the reader to the reviews and monographs [17,20,21,8,15] for details and references. The instability theory by Païdoussis et al. combines the linearized balance of inertia, centrifugal, Coriolis, and elastic forces due to Euler's beam-like deformations in a single equation, assuming that the velocity in the tube is constant. In addition, a connection with the so-called follower-force

* Corresponding author.
E-mail addresses: gaybalma@lmd.ens.fr (F. Gay-Balmaz), putkarad@ualberta.ca (V. Putkaradze).

1631-0721/$ – see front matter
http://dx.doi.org/10.1016/j.crme.2014.01.001

approach, and some lively criticism of the latter, is available in [9]. While this theory had shown good agreement with experiment on some levels [20,11,5], there are several reasons for improvement. For example, that theory, having divergent velocities of disturbances for the short-wavelength limit, is difficult to use for the prediction of long-term dynamics in the unstable regime. In addition, while nonlinear generalizations of the model have been considered [22,21,19,13], it is difficult to consistently extend this approach to include fully nonlinear motion (twist and bend) in three dimensions. Finally, it is difficult to extend this theory to consistently take into account the dynamical change of the cross-section, as we will show below. Some of these drawbacks were addressed in the recent work [2], extending the Kirchhoff rod theory to incorporate the fluid motion inside the tube, and thus being able to predict full 3D motion in linear and weakly nonlinear regime for the case of a *constant* cross-section.

The change of the cross-section caused by the deformations of the tube is the key point of this study. Indeed, the flow of water in a real-life flexible tube can be severely limited or even completely stopped by a sharp bend in the tube. While it is possible to consider a *prescribed* changing cross-section along the tube in the generalization of Kirchhoff's approach, the description of the *dynamical* change of the cross-section has so far been elusive. Previous works have considered the effects of tube narrowing due to stretching [22,21,19,13]. However, the velocity change accommodating the variation of area was considered in the quasi-static approximation for the fluid conservation law, whereas we derive the full evolution equation for velocity. The constriction creates an extra pressure-like term, and this pressure works to undo the bend to its natural position, thus coupling deformation and fluid flow. As it turns out, this effect has an important implication for the instability and, additionally, allows for new nonlinear solutions of traveling-wave type that do not exist for a constant cross-section.

2. Cross-sectional dynamics in fluid conducting tubes

To describe the tube dynamics, we shall use the framework of geometrically exact rod theory [23] which is equivalent to the Kirchhoff rod theory for purely elastic rods. The configuration of the tube deforming in space is defined by: (i) the position of its line of centroids by means of the map $(s,t)\mapsto \boldsymbol{r}(s,t)\in\mathbb{R}^3$, and (ii) the orientation of cross-sections at points $\boldsymbol{r}(s,t)$. The orientation is defined by using a moving orthonormal basis $\mathbf{d}_i(s,t)$, $i=1,2,3$. One possible choice would be to assume that $\mathbf{d}_{1,2}$ are attached to the tube's cross-section (assumed to be a compact set of $\mathbb{R}^2$ with smooth boundary, usually a disk) and the third one normal to that cross-section, but not necessarily parallel to $\boldsymbol{r}_s$. However, other choices of $\mathbf{d}_i$ are possible. The physics, selected by the elastic part of the Lagrangian, selects this basis, defined up to a rigid transform in $SO(3)$ in symmetry-reduced variables. However, for the physically relevant cases, the moving basis is then described by an orthogonal transformation $\Lambda(s,t)\in SO(3)$ such that $\mathbf{d}_i(s,t)=\Lambda(s,t)\mathbf{E}_i$, where $\mathbf{E}_i$, $i=1,2,3$ is a fixed material frame. Note that s is a parameter along the tube and is not necessarily the arc length. The variation of the orientation of the cross-section, i.e. the relative bend or twist, induces a change of the cross-sectional area, i.e., the area of the section of the tube perpendicular to the local centerline in the current configuration. The interior of the tube is filled with an incompressible, inviscid fluid, and we shall approximate the fluid motion by a pure one-dimensional movement from the initial position of the fluid particle S to its current position at time t denoted as $s=\phi(S,t)$. The fluid is thus moving along the tube with the relative velocity $u=\phi_t\circ\phi^{-1}$. The velocity of the rod in space is $\boldsymbol{v}_r=\partial_t\boldsymbol{r}$ and the velocity of fluid is $\boldsymbol{v}_f=\partial_t\boldsymbol{r}+u\partial_s\boldsymbol{r}$, as follows from time differentiating the position of the rod and a fluid particle at s. The physical variables describing the evolution of the rod are the local angular and linear velocities in the rod's frame, $\boldsymbol{\omega}=\Lambda^{-1}\partial_t\Lambda$ and $\boldsymbol{\gamma}=\Lambda^{-1}\partial_t\boldsymbol{r}$, and the corresponding deformations $\boldsymbol{\Omega}=\Lambda^{-1}\partial_s\Lambda$ (Darboux vector) and $\boldsymbol{\Gamma}=\Lambda^{-1}\partial_s\boldsymbol{r}$. These variables satisfy the compatibility constraints that come from equality of cross-derivatives in s and t as:

$$\partial_t\boldsymbol{\Omega}=\boldsymbol{\omega}\times\boldsymbol{\Omega}+\partial_s\boldsymbol{\omega},\qquad \partial_t\boldsymbol{\Gamma}+\boldsymbol{\omega}\times\boldsymbol{\Gamma}=\partial_s\boldsymbol{\gamma}+\boldsymbol{\Omega}\times\boldsymbol{\gamma} \tag{1}$$

In order to incorporate the dynamic change of the cross-section, we assume that the cross-section A is defined by a given instantaneous tube configuration, i.e. is determined by Λ, Λ' and $\boldsymbol{r}'$. Due to the $SO(3)$ invariance of the system, we can posit a function $A=A(\boldsymbol{\Omega},\boldsymbol{\Gamma})$ which we consider arbitrary, but given. The dependence on $\boldsymbol{\Omega}$ comes from the local frame rotating when the tube bends. The dependence on $\boldsymbol{\Gamma}$ comes from the change of cross-section due to stretching. That assumption will break down for the case of a tube with very flexible and easily stretchable walls. If μ is a typical additional pressure generated by the change of A (see below), R is the typical radius of the tube, E is Young's modulus of the tube material, and h the thickness of the wall, then the typical additional deformation is $\delta R\sim\mu R^2/Eh$. For the assumption of A to depend only on the deformations to be valid, and not to be dependent on other variables, we need $\delta R\ll R$, i.e. $h\gg\mu R/E$. For example, for a rubber tube with $R=1$ cm and $\mu\sim 1$ atm, the approximation is valid if $h\gtrsim 10^{-3}$ cm. For comparison, latex balloons and garden hoses have walls $\sim$10 and $\sim$100 times thicker.

With this physical approximation in mind and assuming that the fluid inside the tube is incompressible (in 3D), the volume conservation along the tube reads:

$$Q_t+(Q\,u)_s=0,\qquad Q:=A(\boldsymbol{\Omega},\boldsymbol{\Gamma})|\boldsymbol{\Gamma}| \tag{2}$$

where the extra factor of $|\boldsymbol{\Gamma}|$ appears since s is not assumed to be the arc length. If $A=A(s)$ is independent of t, and $|\boldsymbol{\Gamma}|=\text{const}$, (2) reduces to the conservation law $uA=\text{const}$. This is the equation for velocity used in [22,21,19,13]; however, that approach is inexact as it neglects the time variation of A and stretch $\boldsymbol{\Gamma}$. In addition, setting $u\sim 1/A(\boldsymbol{\Omega})$ in the Lagrangian directly leads to badly posed problems needing an artificial regularization, even in 2D. Recall that the local

velocity of the fluid $u(s,t)$ is measured with respect to the tube. We shall derive all the formulas for an arbitrary dependence of the Lagrangian ℓ on the variables $(\boldsymbol{\omega}, \boldsymbol{\gamma}, \boldsymbol{\Omega}, \boldsymbol{\Gamma}, u)$; however, for the purpose of this paper, we shall use:

$$\ell(\boldsymbol{\omega}, \boldsymbol{\gamma}, \boldsymbol{\Omega}, \boldsymbol{\Gamma}, u) = \frac{1}{2}\int \big(\alpha|\boldsymbol{\gamma}|^2 + \langle \mathbb{I}\boldsymbol{\omega}, \boldsymbol{\omega}\rangle - \langle \mathbb{J}\boldsymbol{\Omega}, \boldsymbol{\Omega}\rangle + \rho A(\boldsymbol{\Omega}, \boldsymbol{\Gamma})|\boldsymbol{\gamma} + \boldsymbol{\Gamma} u|^2 - \lambda|\boldsymbol{\Gamma} - \boldsymbol{\chi}|^2\big)|\boldsymbol{\Gamma}|\,\mathrm{d}s \tag{3}$$

where $\mathbb{I}$ is the local tensor of inertia, α is the linear mass of the tube, ρ is the density of the fluid, and linear elasticity is assumed through the tensor $\mathbb{J}$ and stretch coefficient λ. Here, $\mathbf{E}_i$ is the system of coordinate associated with the material point, with $\boldsymbol{\chi} = \mathbf{E}_3$ pointing along the axis of the tube. More complex elasticity models can be easily incorporated through the general formulas derived below; the key physics in the Lagrangian enters through the kinetic energy of the fluid, i.e. the term proportional to $|\boldsymbol{\gamma} + \boldsymbol{\Gamma} u|^2$.

Theorem 1. *The complete equations of motion for flexible tubes conducting fluid are*

$$\begin{cases} D_t \dfrac{\delta \ell}{\delta \boldsymbol{\omega}} + \boldsymbol{\gamma} \times \dfrac{\delta \ell}{\delta \boldsymbol{\gamma}} + D_s\left(\dfrac{\delta \ell}{\delta \boldsymbol{\Omega}} - \dfrac{\partial Q}{\partial \boldsymbol{\Omega}}\mu\right) + \boldsymbol{\Gamma} \times \left(\dfrac{\delta \ell}{\delta \boldsymbol{\Gamma}} - \dfrac{\partial Q}{\partial \boldsymbol{\Gamma}}\mu\right) = 0 \\ D_t \dfrac{\delta \ell}{\delta \boldsymbol{\gamma}} + D_s\left(\dfrac{\delta \ell}{\delta \boldsymbol{\Gamma}} - \dfrac{\partial Q}{\partial \boldsymbol{\Gamma}}\mu\right) = 0, \quad m_t + (mu - \mu)_s = 0, \quad m := \dfrac{1}{Q}\dfrac{\delta \ell}{\delta u} \end{cases} \tag{4}$$

together with (1) and (2), where $D_t := \partial_t + \boldsymbol{\omega}\times$ and $D_s := \partial_s + \boldsymbol{\Omega}\times$ are the full (material) derivatives.

Proof. The equations of motion are obtained by utilizing the critical action principle:

$$\delta \int \big[\ell(\boldsymbol{\omega}, \boldsymbol{\gamma}, \boldsymbol{\Omega}, \boldsymbol{\Gamma}, u) - \mu\big(Q(\boldsymbol{\Omega}, \boldsymbol{\Gamma}) - \big(Q_0 \circ \varphi^{-1}\big)\partial_s \varphi^{-1}\big)\big]\,\mathrm{d}s\,\mathrm{d}t = 0 \tag{5}$$

in which (2) is imposed with the help of a Lagrange multiplier $\mu(t,s)$ and with respect to the constrained variations [16,10]:

$$\begin{aligned} &\delta\boldsymbol{\omega} = \partial_t \boldsymbol{\Sigma} + \boldsymbol{\omega} \times \boldsymbol{\Sigma}, \qquad \delta\boldsymbol{\gamma} = \partial_t \boldsymbol{\psi} + \boldsymbol{\gamma} \times \boldsymbol{\Sigma} + \boldsymbol{\omega} \times \boldsymbol{\psi}, \qquad \delta u = \eta_t + u\eta_s - \eta u_s \\ &\delta\boldsymbol{\Omega} = \partial_s \boldsymbol{\Sigma} + \boldsymbol{\Omega} \times \boldsymbol{\Sigma}, \qquad \delta\boldsymbol{\Gamma} = \partial_s \boldsymbol{\psi} + \boldsymbol{\Gamma} \times \boldsymbol{\Sigma} + \boldsymbol{\Omega} \times \boldsymbol{\psi} \end{aligned} \tag{6}$$

where $\boldsymbol{\Sigma} = \Lambda^{-1}\delta\Lambda$, $\boldsymbol{\Psi} = \Lambda^{-1}\delta\mathbf{r}$, and $\eta = \delta\phi \circ \phi^{-1}$ are free variations. The expression of the constrained variations follows from the definition of the variables $\boldsymbol{\omega}, \boldsymbol{\gamma}, \boldsymbol{\Omega}, \boldsymbol{\Gamma}, u$ in terms of the Lagrangian variables $\Lambda, \mathbf{r}, \phi$. The minus sign in (5) is chosen so that $\mu(s,t)$ is proportional to the pressure, and not to the negative of pressure. □

Eqs. (1), (2), (4) form a closed system of equations for the tube with moving fluid inside, with the terms proportional to μ describing the effect of the cross-sectional dynamics. Eqs. (4) are valid for an arbitrary function $A(\boldsymbol{\Omega}, \boldsymbol{\Gamma})$ and arbitrary Lagrangians. The precise law $A = A(\boldsymbol{\Omega}, \boldsymbol{\Gamma})$ depends on the material of the tube and its properties. For unstretchable tubes like garden hoses, it is reasonable to put $A = A(\boldsymbol{\Omega})$ and, for small $\boldsymbol{\Omega}$, it is natural to posit $A(\boldsymbol{\Omega}) = A_0 - \frac{1}{2}\boldsymbol{\Omega}^T \mathbb{K}\boldsymbol{\Omega}$, where $\mathbb{K}$ is a symmetric positive definite matrix. We shall additionally assume that this matrix is diagonal $\mathbb{K} = (K_1, K_2, K_3)$ for simplicity. The fact that the area can only decrease with bend and twist can be understood by considering the cross-section to be an ellipse with a given perimeter; a simple geometric consideration shows that the area of this ellipse decreases when the ellipse is deformed away from a circle.

Remark 2. In this paper, we focus on tubes of infinite length. The case of a tube of finite length $0 < s < L$ deserves further important discussions especially concerning the boundary conditions at the free extremity of the tube, that will reported in a future work.

Remark 3. In the equations of motion (4), the motion of elastic material is given by the left-invariant quantities $(\boldsymbol{\omega}, \boldsymbol{\gamma}, \boldsymbol{\Omega}, \boldsymbol{\Gamma})$, since elasticity laws are formulated in the internal body frame. On the contrary, the motion of the fluid is expressed using the right-invariant quantity $u = \phi_t \circ \phi^{-1}$, since the motion is formulated with respect to the (moving) tube. Thus, Eqs. (4) form a mixed system that is neither left nor right invariant.

It is also important to note the effect of viscosity in these considerations. It is common in the works on the subject to neglect the friction effects in the fluid. Indeed, for a $R = 1$ cm tube conducting water at $U = 1$ m/s with the kinematic viscosity $\nu = 0.01$ cm^2/s, the Reynolds number is of the order of $Re = RU/\nu = 10^4 \gg 1$. Thus, the inviscid approximation is justified. For a tube that keeps the elliptical cross-section during dynamics it is possible to incorporate friction in this theory as the friction term coming from the viscous forces, see [18]. This adds a force in the fluid part of the equation depending on $(\boldsymbol{\Omega}, \boldsymbol{\Gamma})$ and U, and an equal and opposite term acting on the tube's walls. In this paper, we shall concentrate on the inviscid theory only; the viscous effects will be considered elsewhere.

In addition to the constriction due to the change of wall geometry, for viscous flows, the curvature of the channel's centerline further affects the flow through Dean's effect [6,7,4], characterized by the parameter $D = 2R\kappa Re^2$, with R being

the radius of the tube, κ the typical curvature and Re is the Reynolds number. Recent studies have also assessed non-steady and non-helical flows [12]. For our case, $D \sim 10^6$–10^8 is so large that no consistent theory is available, although recent studies for smaller, but still high values of D [24] show that for steady flows, appearance of recirculating vortices makes the available cross-section smaller, so the fluid can flow only through a narrow area near the wall.

3. Reduction of motion to two dimensions and linear stability analysis

Let us assume that the tube's motion only occurs in two dimensions, e.g., in the $(\mathbf{E}_1, \mathbf{E}_3)$ plane, with $\boldsymbol{\chi} = \mathbf{E}_3$. In this case, we can define the local inclination of the tube by the angle $\phi(s,t)$. Then, $\Lambda = \exp(\phi \mathbf{E}_2)$ and $(\boldsymbol{\omega}, \boldsymbol{\Omega}) = (\dot{\phi}, \phi')\mathbf{E}_2$. Denoting $K := K_2$, the appropriate eigenvalue of $\mathbb{K}$, we will simply use $A(\boldsymbol{\Omega}) = A_0 - K\boldsymbol{\Omega}^2/2$. Using (3), Eqs. (4) become:

$$\begin{cases} \left(I\phi_t|\boldsymbol{\Gamma}|\right)_t - \left((BK+J)\phi_s|\boldsymbol{\Gamma}|\right)_s + \lambda \boldsymbol{\Gamma} \times \boldsymbol{\chi}|\boldsymbol{\Gamma}| = 0 \\ D_t \dfrac{\delta \ell}{\delta \boldsymbol{\gamma}} + D_s\left(\dfrac{\delta \ell}{\delta \boldsymbol{\Gamma}} - Q\dfrac{\boldsymbol{\Gamma}}{|\boldsymbol{\Gamma}|^2}\mu\right) = 0, \quad B := \dfrac{1}{2}\rho|\boldsymbol{\gamma} + \boldsymbol{\Gamma}u|^2 - \mu \\ \partial_t m + \partial_s(mu - \mu) = 0, \quad m := \dfrac{1}{Q}\dfrac{\delta \ell}{\delta u} = \rho \boldsymbol{\Gamma} \cdot (\boldsymbol{\gamma} + \boldsymbol{\Gamma}u) \end{cases} \tag{7}$$

Instability analysis. While the focus of this paper is on the fully nonlinear dynamics, it is interesting to compare with the linear theory [14,20] to connect to the previous literature. In this paper, for simplicity, we assume that the rod is of infinite length, as the consideration of linear stability of finite rod must follow a more involved procedure, which will be done in future work. For now, let us consider the straight equilibrium $\mathbf{r}_0(s,t) = (s,0,0)$, $\Lambda_0(s,t) = \mathbf{I}$, $u(s,t) = u_0$, $\mu_0(s,t) = 0$, and posit deformations of the form $\mathbf{r}_\varepsilon(s,t) = (s + \varepsilon v(s,t), 0, \varepsilon w(s,t))$, where $\Lambda_\varepsilon(t,s)$ is the rotation with the angle $\varepsilon\phi_1(s,t)$ about the axis $\mathbf{E}_2$. A straightforward calculation shows that v satisfies the wave equation $\alpha\partial_t^2 v - \lambda\partial_s^2 v = 0$, so the motion along the tube is always neutrally stable. The transversal disturbances $w(s,t)$ satisfy:

$$\begin{aligned} &D_1 \cdot D_2 w + \lambda^2 \partial_s^2 w = 0, \qquad D_1 := I\partial_t^2 - \left(\rho u_0^2 K/2 + J\right)\partial_s^2 + \lambda \\ &D_2 := (\alpha + \rho A_0)\partial_t^2 + \left(3/2\rho A_0 u_0^2 - \lambda\right)\partial_s^2 + 2\rho A_0 u_0 \partial_{ts}^2 \end{aligned} \tag{8}$$

The dispersion relation is then obtained by assuming the wave form $w(s,t) = W\mathrm{e}^{\mathrm{i}(ks-mt)}$ and reducing (8) to an algebraic equation $D(m(k),k) = 0$. Because of the assumption of infinite rod, all k are real, for a finite rod the solution to the boundary-value problem leads to complex k. We can obtain this dispersion relation from (8) by $\partial_t \to -\mathrm{i}m$, $\partial_x \to \mathrm{i}k$ and $w \to 1$. Eq. (8) is the analogue of the linear equation considered in [14,20], which in our notation reads:

$$(\alpha + \rho A_0)w_{tt} + \rho A_0 u_0^2 w_{ss} + 2\rho A_0 u_0 w_{st} + J w_{ssss} = 0 \tag{9}$$

It has several similarities and discrepancies, that are important to point out. With no fluid inside, (9) reduces to the Euler beam equation, which has infinite speed of disturbances propagation for $k \to \infty$. In contrast, Eq. (8) reduces to the Timoshenko beam equation, which is consistent for all k. For a finite system, $0 < s < L$, (9) predicts a critical u_0 that depends on the boundary conditions. Our theory gives similar results, except for the case of "strong instability" for all $k > 0$ when $u_0 > U_*$, as explained below. In addition, the stability is strongly altered when the pipe's cross-section is allowed to change, i.e., $K > 0$, which is the key point of this paper.

Theorem 4. *For an infinite tube, the straight configuration is always unstable. There are two cases.*

1. *For $0 < u_0 < U_*$, there is k_* such that for any $0 < k < k_*$, there is at least one unstable branch $m(k)$, i.e., $\mathrm{Im}(m(k)) > 0$, where:*

$$k_*^2 = \frac{(\alpha + \rho A_0)\kappa u_0^2}{J + \frac{1}{2}K u_0^2}, \quad \kappa = \frac{3}{2}\frac{\rho A_0}{\rho A_0 + \alpha} - \left(\frac{\rho A_0}{\rho A_0 + \alpha}\right)^2 > 0 \tag{10}$$

2. *For $u_0 > U_*$, there is at least one branch of $m(k)$ that is unstable for all $k > 0$.*

Proof. We start by rewriting the dispersion relation implicitly (after some considerable algebra) as:

$$k^2(g) = \frac{F(g)}{G_1(g)G_2(g)}, \quad \text{where} \quad \begin{array}{l} F(g) = 2\lambda\left(2(\alpha + \rho A_0)g^2 - 4\rho A_0 u_0 g + 3\rho A_0 u_0^2\right) \\ G_1(g) = 2\alpha g^2 - 2\lambda + 2\rho A_0 g^2 - 4\rho A_0 g u_0 + 3\rho A_0 u_0^2 \\ G_2(g) = 2Ig^2 - \left(2J + K\rho u_0^2\right) \end{array} \tag{11}$$

For any real $k > 0$, the stable solution will have four real roots $g = g(k)$ as given by (11). If these roots are real, the system is stable. The roots are real if and only if the line $k^2 = \text{const}$ intersects the graph of (11) in four distinct points. One can see, however, from analyzing explicit formula (11) that for $k < k_*$ only two solutions exist. The minimum of the function $k^2(g)$ is found analytically, giving (10). For large values of u_0, the equation has only two real roots for any $k > 0$, so at least one

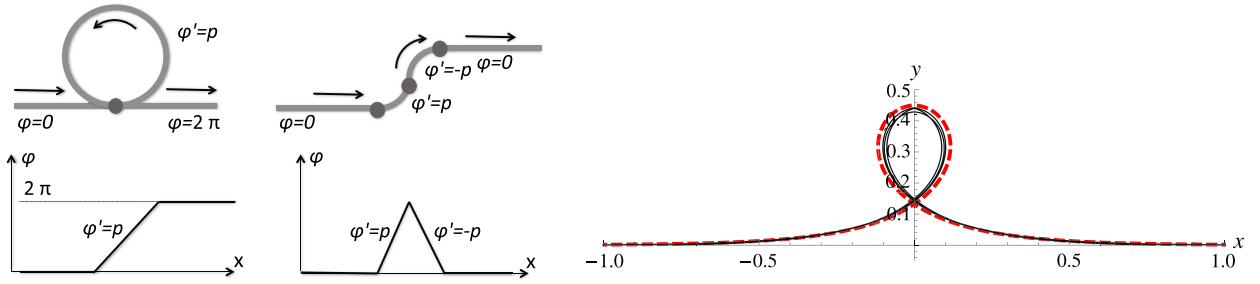

Fig. 1. *Left:* Nonlinear traveling waves: circles (left) and circular arcs (right). Top figure: geometric shape of the tube; bottom figure: $\phi(x)$. *Right:* Three scaled solutions from (14) (solid black lines) for different M (practically indistinguishable) and $M \to 0$ limit (dashed line).

Fig. 1. *Gauche :* Ondes progressives non linéaires : cerles (gauche), arcs circulaires (droite). Figure du haut : configuration spatiale du tube : figure du bas $\phi(x)$. *Droite :* Trois solutions normalisées de (14) (courbes noires continues) pour différents valeurs de M (pratiquement indiscernables) et pour la limite $M \to 0$ (courbe en pointillés).

branch of dispersion relation has $\mathrm{Im}(m(k)) > 0$ (another one will be complex conjugate to that one). The change from two to four roots happens exactly at $u_0 = U_*$ above. □

Note that an infinitely long system is unstable, but the instability of a finite system typically occurs if L is sufficiently large, $k_* \gtrsim 2\pi/L$. A quick estimate shows that for $K = 0$, this estimate is close to the critical value found in [14]. In future work, we will extend that analysis to our system. It is important to emphasize that the important new effect is the change of stability as given by (11), due to cross-sectional dynamics when $K > 0$. If K is large, then $k_* L$ will remain small for all u_0, and the instability will happen through the second case of Theorem 4.

4. Fully nonlinear solutions: traveling waves

In what follows, we derive and analyze exact solutions of (7) of traveling-wave type. Here and below, we will assume inviscid flow for simplicity. If we posit that all variables depend on $x = s - ct$, then $\partial_t = -c\partial_x$ and $\partial_s = \partial_x$. We have the relationships between temporal and spatial variables as $\boldsymbol{\gamma} = -c\boldsymbol{\Gamma}$, $\boldsymbol{\omega} = -c\boldsymbol{\Omega}$, and correspondingly, Eqs. (1) are satisfied automatically. This allows us to eliminate $\boldsymbol{\Omega}$ and $\boldsymbol{\gamma}$ in all equations, keeping only ϕ and $\boldsymbol{\Gamma}$ as variables. Conservation of mass — the fourth equation of (7) — integrates once and gives $Q(u - c) = G = \text{const}$, where G is the volume flux of the fluid. The fluid momentum equation (third equation of (7)) also integrates once, using the boundary conditions $\mu \to 0$ as $x \to \pm\infty$ gives $\mu = \rho G^2 (A(\phi_x)^{-2} - A_0^{-2}) > 0$, so the pressure increases due to deformations. The balances of angular and linear momenta from (7) become, respectively:

$$\big((Ic^2 - (BK + J))\phi_x |\boldsymbol{\Gamma}|\big)_x + \lambda \boldsymbol{\Gamma} \times \boldsymbol{\chi} |\boldsymbol{\Gamma}| = 0, \quad \text{where } B(\phi_x) = \rho G^2 \left(\frac{1}{A_0^2} - \frac{1}{2A(\phi_x)^2} \right) \tag{12}$$

$$\frac{\boldsymbol{\Gamma}}{2|\boldsymbol{\Gamma}|} \left(c^2 I \phi_x^2 + 3\rho \frac{G^2}{A(\phi_x)} - J\phi_x^2 - \lambda |\boldsymbol{\Gamma} - \boldsymbol{\chi}|^2 \right) + \frac{3}{2} \alpha c^2 \boldsymbol{\Gamma} |\boldsymbol{\Gamma}| - \lambda (\boldsymbol{\Gamma} - \boldsymbol{\chi}) |\boldsymbol{\Gamma}| - \mu Q \boldsymbol{\Gamma} |\boldsymbol{\Gamma}|^{-2} = M(\cos\phi, -\sin\phi)^{\mathrm{T}} \tag{13}$$

Here, M is an integration constant having the dimension of energy, and the physical meaning of the absolute value of the momentum flux. Eq. (13) is an algebraic equation for $\boldsymbol{\Gamma}$ for given values of ϕ and ϕ_x. Given the constants (M, G), Eqs. (12)–(13) form a closed algebraic-differential system. Let us now find the solutions of these equations for arbitrary M.

Lemma 5 *($M = 0$ case). Eq. (13) with $M = 0$ only has weak solutions for $\phi(x)$, which are piecewise linear functions in x, consisting of $\phi_x(x) = 0$ and $\phi_x(x) = p = \text{const}$ defined from $B(p)K = Ic^2 - J$, with $B(p)$ given by (12).*

Proof. When $M = 0$ in (13), we see that $\boldsymbol{\Gamma}$ must be parallel to $\boldsymbol{\chi}$. Multiplying this equation by an arbitrary test function $v(x)$, integrating from $x = -\infty$ to $+\infty$ and performing one integration by parts, we get $\int_{-\infty}^{\infty} (Ic^2 - (B(\phi_x)K + J))\phi_x |\boldsymbol{\Gamma}| v_x = 0$, where we have used $\phi \to 0$ as $x \to \infty$. Since $v(x)$ is arbitrary, all the weak solutions are given by $\phi_x = 0$ or $\phi_x = p = \text{const}$, with p satisfying $B(p)K = Ic^2 - J$. □

Note that the solution with $\phi'(x) = p = \text{const}$ forms a circular arc. These solutions can be put together in arbitrary combinations, the simplest one being a propagating circle connecting to two straight lines as illustrated in the left part of Fig. 1. Once $\phi(x)$ is determined, $\boldsymbol{\Gamma}(x) = \Gamma(x)\boldsymbol{\chi}$ is computed from the algebraic equation (13).

If $M \neq 0$ in (13), further exact analytical progress is difficult. While it is possible to solve the system as differential-algebraic equations, we make the physical assumption that due to high stretch resistance of the rod, i.e. $\lambda \gg 1$, the

stretching is small. Using the asymptotic expansion of $\boldsymbol{\Gamma}$ in $1/\lambda$ around $\boldsymbol{\chi}$, and inserting it in (13), we obtain that $\boldsymbol{\Gamma}\cdot\mathbf{E}_1 = \lambda^{-1}M\sin\phi + o(\lambda^{-1})$. Thus, Eq. (12) (up to order $o(\lambda^{-1})$) becomes:

$$\left(\left(Ic^2 - \left(B(\phi_x)K + J\right)\right)\phi_x\right)_x - M\sin\phi = 0 \tag{14}$$

It is possible to find exact solutions of (14) in quadratures. We do not present this solution here, but plot several scaled solutions (see below) on the right-hand part of Fig. 1. As it turns out, there is a universal shape describing these solutions after proper scaling with a high accuracy for arbitrary $M \neq 0$.

Assume that $M > 0$; if $M < 0$, the change $\phi \to \phi + \pi$ reverses the direction of the flow and reflects the solution about the x-axis, changing $M \to |M| > 0$. In the limit $M \to 0$, when the loop becomes very large and the change of $\phi(x)$ is slow, under rescaling $x \to X/\sqrt{M}$, $\phi_x \to \sqrt{M}\phi_X \to 0$ and $B(\phi_x) \to B(0) = B_0$, so (14) assumes the limiting form with $M = 1$ and $A = A_0$. To illustrate this, the right-hand part of Fig. 1 shows the collapse of scaled spatial solutions of (14) to a single shape, well approximated by the universal solution shown with a dashed line.

It is worth noting that when the cross-section of the tube is constant, i.e. $K = 0$, the only solutions with $M = 0$ are $\phi = 0$. The solutions with $M \neq 0$ preserve their loop-like appearance and scaling, but are different from those discussed here. Traveling solutions for the inextensible and unshearable rod can be found as well, giving exactly (14). Thus, the solutions in the limit of $\lambda \to \infty$ converge to those of inextensible and unshearable rod, as expected.

We shall also mention that a simple physical model can be constructed as an elastic chain of heavy rigid tubes with the fluid velocities depending on the relative orientation between the neighboring tubes. Even for two links, such a model shows a highly non-trivial behavior, overcoming the stabilizing effects of gravity and elasticity. These models will be described in more details in our future work.

Acknowledgements

We acknowledge useful discussions on experiments with Mitchell Canham and David Nobes, and on mathematical theory with Darryl Holm, Tudor Ratiu, Michael Tabor and Cesare Tronci. VP acknowledges support from NSERC Discovery, NSF Grant No. DMS-0908755 and from the DTRA Joint Science and Technology Office (Grant No. HDTRA1-10-1-0070). FGB is partially supported by a “Projet Incitatif de Recherche” (ENS, Paris).

References

[1] H. Ashley, G. Haviland, J. Appl. Mech. 17 (1950) 229–232.
[2] M.A. Beauregard, A. Goriely, M. Tabor, Int. J. Solids Struct. 47 (2010) 161–168.
[3] T.B. Benjamin, Proc. R. Soc. A 261 (1961) 457–486.
[4] S.A. Berger, L. Talbot, L.S. Yao, Annu. Rev. Fluid Mech. 15 (1983) 461–512.
[5] A. Cros, J.A.R. Romero, F.C. Flores, Sky Dancer: A Complex Fluid–Structure Interaction, Experimental and Theoretical Advances in Fluid Dynamics: Environmental Science and Engineering, Springer, 2012, pp. 15–24.
[6] W.R. Dean, Philos. Mag. 4 (1927) 208–223.
[7] W.R. Dean, Philos. Mag. 5 (1928) 673–695.
[8] O. Doaré, E. de Langre, Eur. J. Mech. A Solids 21 (2002) 857–867.
[9] I. Elishakoff, Appl. Mech. Rev. 58 (2005) 117–142.
[10] D. Ellis, D.D. Holm, F. Gay-Balmaz, V. Putkaradze, T. Ratiu, Arch. Ration. Mech. Anal. 197 (2010) 811–902.
[11] F.C. Flores, A. Cros, J. Phys. Conf. Ser. 166 (2009) 012017.
[12] D. Gammack, P. Hydon, J. Fluid Mech. 433 (2001) 357–382.
[13] M.H. Ghayesh, M.P. Païdoussis, M. Amabili, J. Sound Vib. 332 (2013) 6405–6418.
[14] R.W. Gregory, M.P. Païdoussis, Proc. R. Soc. A 293 (1966) 512–527.
[15] R.W. Gregory, M.P. Païdoussis, Proc. R. Soc. A 293 (1966) 528–542.
[16] D.D. Holm, V. Putkaradze, C. R. Acad. Sci. Paris Ser. I 347 (2009) 1093–1098.
[17] M.P. Païdoussis, G.X. Li, J. Fluids Struct. 7 (1993) 137–204.
[18] H. Lamb, Hydrodynamics, 6th ed., Dover, 1932.
[19] Y. Modarres-Sadeghi, M.P. Païdoussis, J. Fluids Struct. 7 (2009) 535–543.
[20] M.P. Païdoussis, Fluid–Structure Interactions. Slender Structures and Axial Flow, vol. 1, Academic Press, London, 1998.
[21] M.P. Païdoussis, Fluid–Structure Interactions. Slender Structures and Axial Flow, vol. 2, Academic Press, London, 2004.
[22] C. Semler, G.X. Li, M.P. Païdoussis, J. Sound Vib. 169 (1994) 577–599.
[23] J.C. Simó, J.E. Marsden, P.S. Krishnaprasad, Arch. Ration. Mech. Anal. 104 (1988) 125–183.
[24] L. Zabielski, A.J. Mestel, J. Fluid Mech. 370 (1998) 297–320.